Observing individual fish behavior in fish aggregations: Tracking in dense fish aggregations using a split-beam echosounder

Nils Olav Handegard[a)]
Institute of Marine Research, Bergen, Norway

(Received 2 May 2006; revised 5 April 2007; accepted 21 April 2007)

Acoustic instruments are important tools for observing the behavior of aquatic organisms. This paper presents a simple but efficient method for improving the tracking of closely spaced targets using a split-beam echosounder. The traditional method has been a stepwise approach from the detection of echoes, rejection of apparently multiple targets and then tracking the remainder. This is inefficient because the split-beam angles are not included in the initial detection; rather they are only used in the rejection criteria before the subsequent tracking. A simple track-before-detection method is presented, where the phase angles, echo intensities, ranges, and times are used simultaneously, resulting in better detection and tracking of the individual fish. Two test data sets were analyzed to determine the effectiveness of this method at discriminating individual tracks from within dense fish aggregations. The first data set was collected by lowering a split-beam transducer into a herring layer. The second data set, also collected with a split-beam transducer, was from a caged aggregation of feeding herring larvae. Results indicate the potential of target tracking, using a split-beam echosounder, as a tool for understanding interindividual behavior. © *2007 Acoustical Society of America.* [DOI: 10.1121/1.2739421]

PACS number(s): 43.30.Sf [KGF] Pages: 177–187

I. INTRODUCTION

Ecosystem studies depend on knowledge of the individual components. Several studies have shown the feasibility of using various acoustic methods for measuring the behavior of individual targets *in situ*, both for fish (Arrhenius *et al.*, 2000; Torgersen and Kaartvedt, 2001) and plankton (Jaffe *et al.*, 1999; Klevjer and Kaartvedt, 2003). A particularly nice example is Genin *et al.* (2005), where the observed swimming behavior of zooplankton relative to water currents has been used to explain the observed aggregation patterns. Among other acoustical studies concerning the behavior of individuals are the behavior of over-wintering herring in the Ofotfjord (Huse and Ona, 1996), vertical search patterns in fish (Cech and Kubecka, 2002), diel differences in swimming patterns in fish (Gjelland *et al.*, 2004) and zoo-plankton (De Robertis *et al.*, 2003), behavioral changes induced by a trawling vessel (Handegard *et al.*, 2003; Handegard and Tjøstheim, 2005), and the feasibility for devices to prevent fish entering hydroelectric turbine intake (McKinstry *et al.*, 2005). McQuinn and Winger (2003) used manual tracking to investigate the impact of diel-dependent fish behavior on target strength. Riverine and shallow-water research is another large field where acoustic methods have been used to observe fish behavior, with special emphasis on migratory behavior and counting (Enzenhofer *et al.*, 1998; Mulligan and Chen, 1998; Mulligan and Kieser, 1996). This interest is motivated by the fact that echo integration is difficult to apply in a riverine environment.

Schooling behavior is a spectacular pattern in nature, and there have been many attempts to uncover the dynamics of this phenomenon. Parr (1927) introduced the idea of simple repulsive and attractive "forces" between individuals, and these ideas were further developed by Breder (1954) and Sakai (1973). The first individual-based data simulation was reported by Aoki (1982). Similar model approaches have been described by Reynolds (1987) and Huth and Wissel (1992). All these models demonstrate that simple rules on the individual can result in complex school dynamics. However, data to support these models are scarce, and methods capable of quantifying interindividual behavior are needed, in particular for closely spaced individuals. The latter problem is the main motivation for the present study, but the method is general and is also useful for other tasks involving the detection of single individuals, e.g., target strength measurements. The goal of this work, therefore, is to develop an improved method for tracking closely spaced individual targets using split-beam echosounders.

A. The state of the art

Two different acoustic instruments for observing behavior are the multibeam sonar, see, e.g., Jaffe *et al.* (1995), and the split-beam echosounder (Brede *et al.*, 1990; Ehrenberg and Torkelson, 1996). The multibeam sonar can handle several targets at a given range, but the resolution is limited by the number of beams and their opening angles. There are, however, methods to compensate for this problem (Jaffe, 1999; Schell and Jaffe, 2004), but at the cost of being able to observe fewer animals at the same range. The somewhat simpler split-beam echosounder is ineffective when multiple targets are located at the same range (Foote, 1996). The split-

[a)]Electronic mail: nils.olav.handegard@imr.no

beam echosounder does not depend on the grid-cell volume in the same way as the multibeam sonar, but it needs a fair signal-to-noise ratio to work properly (Kieser *et al.*, 2000). Both methods have limitations when observing dense aggregations of targets. This study focuses on the use of split-beam echosounders because of their relative simplicity and availability to researchers.

The split-beam echosounder transmits an echo pulse into the water column, and the backscattered signal is received on four quadrants of the transducer face. The phase differences between the four quadrants are used to estimate the direction to the target, so each sample (or pixel in the echogram) is associated with an intensity and two angles, in addition to the receive time and corresponding range as given by the location in the echogram. If there is a single target at a given range, the angles are representative of the position of that target. However, if there is no target or there are multiple targets at the same range, the angles do not represent the position of a single target. It is thus not possible for two fish at the same range to provide valid observations.

Traditionally, obtaining target tracks from acoustic data has been a two-step process (Ehrenberg and Torkelson, 1996, p. 329). First, the targets are detected with a single-echo-detection (SED) algorithm, and then these detections are combined into tracks making use of their positions in successive pings. The potential of this method for observing fish behavior has been acknowledged for a long time (Foote *et al.*, 1986, 1984; Ona, 1994). In general, target tracking is a well-established field, see, e.g., Blackman and Popoli (1999), and has been further developed for split-beam data (Handegard *et al.*, 2005; Xie, 2000).

The SED targets were originally used to estimate the target strength (TS) of the individual fish within the echo beam (Brede *et al.*, 1990; Foote *et al.*, 1986, 1984; Ona, 1999). For this purpose, it is crucial to avoid two targets being considered as one since this would positively bias the results (Foote, 1996). Different methods to reject SED targets contaminated with multiple targets include the use of phase, amplitude, and echo-duration information from the returned echo, see Soule *et al.* (1996) for an evaluation of these methods. When successful, the results of SED algorithms are high-quality targets with corresponding estimates of TS and location in the beam. However, the SED algorithms are not designed for tracking purposes, and there are often missing pings within a track due to the strict SED rejection criteria. The SED algorithm works on ping-by-ping data, and little effort has been applied to use the temporal dimension of the data to improve single-echo detection. One exception is Balk and Lindem (2000), who use the information in adjacent samples (range and time) to decide whether a sample in the echogram belongs to a target or not, a technique known as cross-filter detection which is used to aid the SED algorithm. This, along with other tracking tools, is implemented in the SONAR 5 software (SONAR 5 user manual, Helge Balk, University of Oslo, Norway). The idea of using the temporal dimension is intellectually appealing, since it utilizes information that "conventional" detectors discard. The SONAR 5 software can also interpolate sample data between already-detected SED targets, leading to better tracking performance than conventional methods.

B. Posttracking detection

In this paper, the target angles, echo intensity, time, range, and the actual tracking results are considered in one single step. It is not based on the traditional stepwise process of detection, rejection, and tracking, where the angles are used as rejection criteria only, and single targets must be passed by the SED algorithm to initiate tracks. The idea is inspired by the track-before-detect approach (Blackman and Popoli, 1999, p. 18). In order to achieve this, all samples above a threshold are initially treated as single targets. Note that a target is typically composed of several samples. The threshold is set lower than the expected intensity of the target echoes, ensuring that no targets are lost. Consequently, low intensity samples where no fish are present are treated as valid targets. Each sample has its own apparent position and intensity. The range and time are determined by the sample (pixel) position in the echogram, while the angles and intensities are given by the pixel values in the echogram and "anglegrams,"[1] respectively. The low threshold results initially in many false targets, but the advantage is that no information is lost in this initial step, as opposed to the traditional approach, where the SED algorithm rejects many targets. This calls for a different approach when associating samples to tracks, by postponing the quality screening until the tracks have been established, which may be denoted "track rejection" as opposed to the single-target rejection applied in the SED algorithm. The main objective of this paper is to develop these techniques.

II. MATERIALS AND METHOD

This section is divided into three main parts. First the test data sets are presented. The second part is the actual method of data association, i.e., associating samples to tracks. Finally the track rejection and track quality algorithms are described. The other aspects of the tracking, like track estimation, incorporating platform movement, etc., are the same as described in Handegard *et al.* (2005). That paper is somewhat technical, and it is not necessary to fully understand the details there to appreciate the ideas presented here. However, track estimation is an important part of any tracking system, and therefore a paragraph in Sec. IV briefly addresses these questions.

A. Test data

Test data set I [see Figs. 1(a)–1(d)] was obtained by a Simrad EK60 split-beam echosounder with a Simrad 38DD, a 38-kHz, 7°-beamwidth circular transducer. This transducer is depth stabilized and certified to be used down to 1500 m depth. The test set is taken looking horizontally into a herring (*Clupea harengus*) layer. The reason for aligning the sounder horizontally was originally to investigate the horizontal-aspect TS for herring, but it is also the preferred orientation when observing interindividual fish behavior, since there are indications that the fish will orientate relative to the neighboring fish horizontally more so than vertically

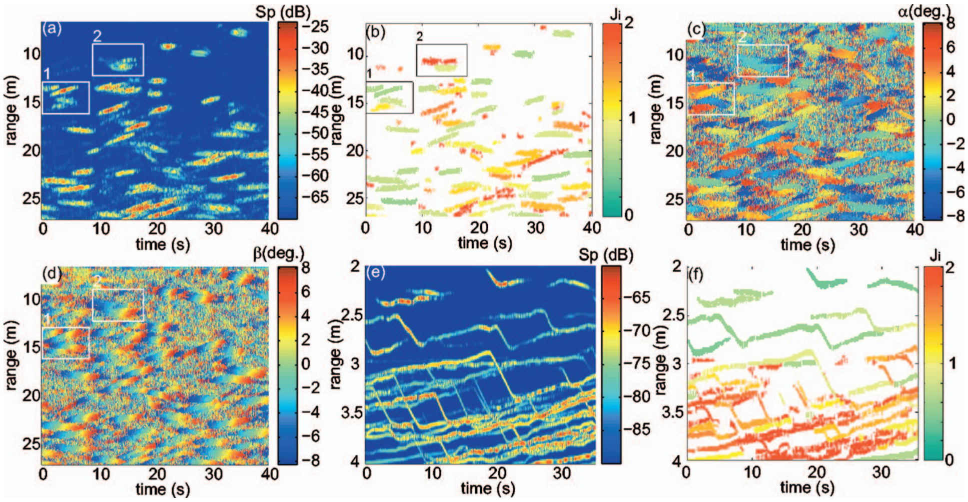

FIG. 1. (a) The example echogram for data set I. The echogram is given in S_p (dB re m^2) units. The boxes labeled 1 and 2 are the subsets 1 and 2, which are used as examples of successful and unsuccessful tracking, see Figs. 4 and 5, respectively. (b) The track quality for each track, J_i, where red indicates rejected tracks ($J_i > 1$) and green indicates accepted tracks ($J_i \leq 1$). Tracks with $J_i > 2$ are shown as $J_i = 2$. (c), (d) The corresponding alongship and athwart ship angles, respectively, in degrees. (e) The echogram for data set II and (f) the resulting quality of the tracks in test data set II, J_i.

(Grünbaum)^2. The range of the probing echosounder was set to 27 m allowing for a very high ping rate of 17 Hz. In addition the sample interval was set to 9.4 cm with a pulse duration time τ of 512 μs. The output power P_t was set to 200 W. All data recorded closer than 6 m were discarded due to near field effects. The received power was converted to $S_p = 10\log(s_p)$ with unit dB re m^2, where

$$s_p = \frac{P_{r,i} 16\pi^2}{P_t g_0^2 \lambda^2} r_i^4 10^{2\alpha r_i}.$$

Here P_t is the output power, g_0 is the on axis gain, λ is the wavelength, α is the absorption coefficient, $P_{r,i}$ is the received power in sample i, and r_i is the corresponding range. In fisheries acoustic terms, this corresponds to time varied gain (TVG) of 40 log r and no beam pattern compensation.

Test data set II [see Figs. 1(e) and 1(f)] was obtained by a Simrad EK60 Split-beam echosounder with a Simrad ES 200-7C, a 200-kHz, 7°-beamwidth circular transducer, looking vertically into a cylindrical container of black polyethylene sheeting. The aim of this experiment was to investigate feeding behavior of herring larvae in a wide and physically controlled volume of sea water (a mesocosm). The bag was supported by ropes attached to a stainless steel circular ring connected to an open raft in a sheltered bay. The bag and the raft constituted a single entity floating on the sea surface. The pulse duration time τ was 64 μs, with a corresponding sample interval of 1.2 cm, and a ping rate of 16.8 Hz. The output power P_t was set to 1000 W.

In order to compare the present method to the original SED algorithm, single targets are detected in test data set I by the SED algorithm incorporated in the EK60 and by the SONAR 5 software. The echo-length acceptance criteria are set wide and the phase deviations high in order to reject less targets (Table I).

B. The method

Since the sample data are being used directly, no prior detection is necessary. The idea is that samples are treated as targets and that several samples from the same ping may be associated with the same single target, somewhat similar to the concept of joint probabilistic data association (Blackman and Popoli, 1999, pp. 353–355), but probabilities of detection are not considered and multiple samples may not be shared by two tracks.

A tracking system consists of several steps, including track estimation, track prediction, gating, data association, and track support. Gating, data association, and track support are presented in detail in the following, but track estimation and track prediction are only summarized. The details are presented in Handegard *et al.* (2005).

Prior to tracking, a threshold is set to initially remove samples not being targets. This threshold is set low to ensure that weak targets are not missed in the subsequent algorithm. The thresholds for data sets I and II are −70 and −90 dB, respectively, and are set based on visual inspection of the echograms [Figs. 1(a) and 1(e)] with different thresholds.

Each sample above the threshold is treated as an observation, and consists of $\mathbf{y} = [\alpha\ \beta\ r\ I]$, where α and β are the alongship and athwartship angles, respectively, r is the range, and I is the energy of the sample. The intensity measure used here is S_p.

TABLE I. The EK60 and SONAR 5 single-echo-detection (SED) settings for the case I test set. The parameters are chosen to allow more detections than the typical settings. The "echo lengths" are given as a factor multiplied with the pulse duration time τ. Maximum phase deviation is the maximum allowed average electrical phase jitter between samples inside an echo from a single target. For the echosounder and transducer used here (case I), one phase step corresponds to 0.064°. The recommended setting for weak targets is four to ten phase steps. Maximum gain compensation is the correction value from the one-way model of the transducer beam pattern. For the Simrad 38DD transducer, this corresponds to a maximum acceptable off-axis angle of ~5°. The threshold is applied to the echogram in S_p (dB re m^2) units.

	EK60	SONAR 5
Software version	1.4.4.66	v5.9.6
Minumum echo length (s)	0.2τ	0.2τ
Maximum echo length (s)	2.7τ	2.7τ
Maximum phase deviation (phase steps)	10.0	23.0
Maximum gain compensation (dB)	6.0	6.0
Threshold (dB)	−50	−50
Multiple peak suppression	N/A	Off
Min distance between detections (cm)	N/A	1

TABLE II. The tracking parameters for data set I and data set II: The threshold (TH), the gate parameters (α_g, β_g, r_g, and I_g), the track initiation parameters (α_0, β_0, r_0, I_0, and N_0), the track termination parameters, including the maximum within gate conflicts (N_c), the maximum number of missing samples between the first and last sample in range (N_e), the maximum number of successive missing pings (N_m), and the track rejection parameters, including the missing pings to track-length ratio (NM), the track length (TL), and the samples to track length ratio (NL).

	TH (dB)	α_G β_G (deg)	r_G (m)	I_G (dB)	α_0 β_0 (deg)	r_0 (m)	I_0 (dB)	N_0	N_c	N_e	N_m	MN	TL	NL
Data set I	−70	2.80	0.44	20	2.80	0.12	20	5	3	2	1	0.80	8	2.00
Data set II	−90	1.80	0.10	20	2.00	0.03	20	5	2	2	1	0.80	8	2.00

At each time step, the track state $\mathbf{x}$ (position, velocity, and echo intensity) for each live track is estimated using a Kalman filter, and assuming constant velocity, the state is predicted at the next time step [Handegard *et al.*, 2005, their Eq. (5)]. The predicted state is denoted $\tilde{\mathbf{x}}$.

To compare predictions with observations, the predicted state $\tilde{\mathbf{x}}$ is mapped to observation space, i.e., $\tilde{\mathbf{x}} \rightarrow \tilde{\mathbf{y}}$. For the position, this involves mapping the Cartesian position of the track to alongship angle, athwartship angle, and range [Handegard *et al.*, 2005, their Eq. (4)]. The velocity is not part of the mapping, and the echo intensity is the same in both spaces. This allows us to define a distance metric between a sample $\mathbf{y}$ and a live track $\tilde{\mathbf{y}}$ (predicted position in observation space). The metric is the so-called gate distance defined in the following.

1. Gating

The first part of the data association is the gating. This decides which samples should be considered to be parts of the track. In the following, i, j, and k denote track number, sample number, and ping number, respectively. The difference between the prediction from track i and sample j is calculated for all predictions and samples at ping k, i.e.,

$$\hat{\boldsymbol{\epsilon}}_{ijk} = \mathbf{y}_{jk} - \tilde{\mathbf{y}}_{ik}. \tag{1}$$

The gate distance

$$d_{ijk} = \hat{\boldsymbol{\epsilon}}_{ijk} G \hat{\boldsymbol{\epsilon}}_{ijk}^T \tag{2}$$

is a measure of closeness between samples and predictions. If $d_{ijk} \leqslant 1$, sample j is inside the gate of track i at ping k. Here T is matrix transpose and

$$G = \begin{bmatrix} \alpha_G^2 & 0 & 0 & 0 \\ 0 & \beta_G^2 & 0 & 0 \\ 0 & 0 & r_G^2 & 0 \\ 0 & 0 & 0 & I_G^2 \end{bmatrix}^{-1}. \tag{3}$$

Note that the intensity is also included in the gate. The elements in G are set as parameters in this case, α_G, β_G, r_G, and I_G being the maximum allowed deviances between the observation and the prediction along each dimension (see Table II). This means that if the maximum deviation occurs in α, no deviance is allowed in any of the other dimensions. Consequently, the maximum deviance rarely occurs. The interpretation is that the observation must be within a hyperellipsoid defined by $d \leqslant 1$ (see Fig. 2). There are ways to set the gate parameters based on detection probabilities and innovation covariances, i.e., the covariance of $\hat{\boldsymbol{\epsilon}}$, but this is not done here, cf. the discussion to follow.

2. Data association

The next step is to associate the samples inside the gates to tracks. At each ping a gate is calculated for each live track, but a given sample may be inside more than one gate, and a given gate may contain more than one sample. If there are no conflicts, i.e., no samples lie within more than one gate, each sample is associated to the corresponding track. If there are conflicting observations, they are associated to the "closest" track in terms of d. However, if the number of conflicting observations inside a gate is higher than the *ad hoc* parameter N_c, the shortest track is automatically terminated. In general the N_c parameter is a crude method to avoid wrong associations, and tuning the gates are preferred over decreasing N_c. The result of the data association step is that each sample j at ping k that are deemed part of a track i is associated with track number i. The set of samples j associated with track i at ping k is denoted A_{ik}. Similarly, the set A_i is defined as the set of all samples associated with track i over the full duration of the track.

The observations j that are associated to track i at ping k are then combined into a composite observation by

$$\mathbf{y}'_{ik} = \frac{\sum_{j \in A_{ik}} w_{ijk} \mathbf{y}_{jk}}{\sum_{j \in A_{ik}} w_{ijk}}, \tag{4}$$

where $w_{ijk} = \exp(-d_{ijk}^2)$. This weighted observation is used in the Kalman update equation. This approach is analogous to joint probabilistic data association, where the weights are

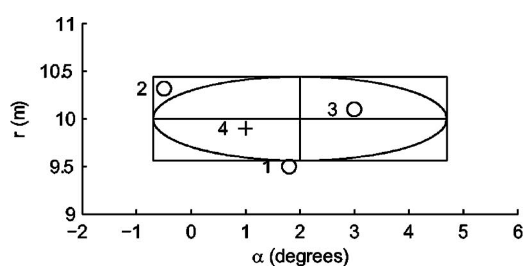

FIG. 2. Two-dimensional projection of the four-dimensional gating process; the center of the ellipsoid is the prediction by the Kalman filter algorithm. Four samples are given for illustrative purposes. Sample 1 is outside the range gate r_G, sample 2 is inside the range of r_G and α_G separately (illustrated by the rectangle), but outside the ellipsoidal gate since the deviations are summed. Sample 3 is inside the gate of r_G and α_G (illustrated by the ellipse), but the gate is four dimensional, and this sample lies outside the ellipsoidal gate, because of a large offset in β. Finally, sample 4 lies within the ellipsoidal gate and is associated with the prediction.

determined by closeness to the prediction, but detection probabilities are not considered here. The updated state variables are used to obtain predictions for the next time step, and then the process is repeated.

3. Initiating and terminating tracks

Before proceeding to the next time step, samples not associated with tracks are used as candidates for new tracks. Initiating new tracks is difficult since there are usually several sample values for each new target. The method chosen for initiating new tracks is similar to the tracking of already established tracks. The nonassociated samples within a ping are compared in pairs (each sample is paired with the next adjacent sample). By taking the first sample as a prediction and the second as an observation, Eqs. (1) and (2) can be used to calculate the distance between them, using the track-initiation gate

$$G_0 = \begin{bmatrix} \alpha_0^2 & 0 & 0 & 0 \\ 0 & \beta_0^2 & 0 & 0 \\ 0 & 0 & r_0^2 & 0 \\ 0 & 0 & 0 & I_0^2 \end{bmatrix}^{-1} \tag{5}$$

instead of the regular gate. If the difference between these samples is less than unity, i.e., the second is within the gate of the first, the second sample is compared with the next adjacent sample is range, etc., forming a chain of samples that are within each other's gates. When a sample does not fall within the gate of the previous, the chain is determined. If the length of the chain is larger than N_0, a new track is formed based on the mean of these samples. If many adjacent samples (in range) meet the criteria, there is a possibility for combining several new targets into one, and this will occasionally happen. Several tools have been developed to remove or to flag these tracks as low-quality results, cf. Sec. II C.

Track termination is the method applied to close a track during tracking. Three methods for track termination are implemented. The gate-conflict parameter N_c has already been defined as the maximum number of conflicting targets within a gate. Furthermore, when tracking very weak targets, the background reverberation may be tracked. These "tracks," however, typically have several missing samples within them. To terminate these tracks, the number of missing samples between the first and last sample (in range) are counted, and if they exceed N_e samples, the track is terminated. Finally, the number of successive missing pings, N_m, is used. However, after a track is terminated, other techniques can be used to test its quality or to reject it, cf. Sec. II C.

C. Quality control

When tracking fish in dense registrations, misassociations and track-split errors will inevitably occur, and a method to reject or to flag each track with an association-quality measure is important. The track quality algorithm is based on measures of association errors, and the track rejection algorithms are based on more *ad hoc* criteria. The criteria adopted for rejecting tracks are simply the number of missing pings to the track length ratio (MN) the track length (TL), and the total number of samples to the track length ratio (NL). These are set as parameters.

Previously, association errors have been investigated for single targets, i.e., false or missing associations between single detections (Handegard *et al.*, 2005, see, e.g., their Sec. III D). However, that measure cannot be used here because target detection and tracking are not separated. Since the algorithm presented here works on samples, misassociation in range may also occur, both as connection errors (one track may consist of several fish) and track-split errors (several adjacent tracks may be formed from one single fish). Four measures of track quality have been defined. The first two measures take a global approach where no particular misassociation type is addressed, whereas the two last measures deal with track connection and track-split errors in range, respectively.

One way to investigate association errors is to compare the results from a forward and backward run through the data set. If questionable associations have occurred, it is likely that a different result would be obtained by running the data association backwards, i.e., starting from the end of the data set and progressing to the beginning. For a given track in the primary data set, e.g., the forward run, the samples associated with track i are given by A_i. Let B_l be the set of samples associated with track l from the backward run. The intersection is given by $A_i \cap B_l$, and let N_{A_i}, N_{B_l}, $N_{A_i \cap B_l}$ be the number of samples in the respective sets. Two measures comparing the backward and forward runs are defined. Let

$$J_{a,i} = 1 - \max_l (N_{A_i \cap B_l})/N_{A_i}. \tag{6}$$

This results in a measure of how well the "best" backward track overlaps the forward track, and the identifier l for that track. The range of J_a is $[0\ 1]$, where a high value indicates that the forward track contains false associations or the backward track is split. Let

$$J_{b,i} = 1 - (N_{A_i \cap B_l})/N_{B_l}, \tag{7}$$

where l is the backward track that maximized $N_{A_i \cap B_l}$ in Eq. (6). Again the range is $[0\ 1]$, and a high J_b value indicates the occurrence of track-split errors in the forward track or false association in the backward track. Since the index l is taken from Eq. (6), J_a do not necessarily become J_b when using the backward run as the forward run. This procedure is illustrated in Sec. III on a subsample of the test data set I, cf. Fig. 5.

The track initialization algorithm may be stricter than that used to continue an already initiated track; one result of this could be a late initiation of tracks. By combining high-quality-forward and backward tracks in terms of J_a and J_b, the dependence on track initiation parameters may be reduced. The new track is defined by the union $A_i \cup B_l$ of the matched tracks. If weak targets along the edges of the tracks are a concern, the intersection between the forward and backward track, $A_i \cap B_l$, can be used instead.

A track-split error may occur if the tracks are initiated incorrectly, i.e., when two tracks are initiated for one fish, or if the gates from two tracks cover the same samples. This can be observed in the echogram as two adjacent tracks, where the tracks are not separated by any nonassociated samples. A measure to detect this effect is simply to check the sample above and below the track. If that sample belongs to another track, a track-split error may have occurred, i.e.,

$$J_{\text{split},ik} = \frac{N_a}{2}, \tag{8}$$

where $N_a \in \{0,1,2\}$ if there is, or not, an adjacent track above, below, or both at ping k for track i. The factor $1/2$ is for scaling the measure to the range [0 1]. For the whole track

$$J_{\text{split},i} = \frac{1}{L_i}\sum_{k}^{L_i} J_{\text{split},ik}, \tag{9}$$

where L_i is the length of the track (excluding missing pings).

A track merging error in range occurs when one track is formed from two fish, e.g., if the initiation and tracking gates are set too wide. It is desirable to set the gates wide to capture rapid changes in behavior, but at the possible cost of misassociation, both in range and time. However, using standard SED rejection criteria, misassociations in range can be monitored. Following the recommendations of Soule *et al.* (1996) for successful multiple-target rejection in SED algorithms, the phase angle deviation over one target in one ping is calculated as a measure of track-combination error in range, i.e.,

$$J_{\text{merge},ik} = \frac{1}{2}\left[\frac{1}{N_{A_{ik}}-1}\sum_{j\in A_{ik}}(\bar{\alpha}_{ik}-\alpha_{jk})^2\right]^{1/2} + \frac{1}{2}\left[\frac{1}{N_{A_{ik}}-1}\sum_{j\in A_{ik}}(\bar{\beta}_{ik}-\beta_{jk})^2\right]^{1/2}, \tag{10}$$

where $N_{A_{ik}}$ is the number of samples for track i at ping k and $\bar{\alpha}_{ik}$ and $\bar{\beta}_{ik}$ are the mean athwartship and alongship angles for track i and ping k, respectively. To use this measure for each track i,

$$J_{\text{merge},i} = \max_k (J_{\text{merge},ik}) \tag{11}$$

is defined. The maximum value is chosen since one erroneous association can severely bias the velocity estimate for the whole track. For applications where false associations are of less concern, the mean value could be used instead.

Four measures of quality control have been described. Each of these can be monitored individually, or they can be scaled relative to each other like

$$J_i = \left\{\left(\frac{J_{\text{a},i}}{J_{\text{a},0}}\right)^2 + \left(\frac{J_{\text{b},i}}{J_{\text{b},0}}\right)^2 + \left(\frac{J_{\text{merge},i}}{J_{\text{merge},0}}\right)^2 + \left(\frac{J_{\text{split},i}}{J_{\text{split},0}}\right)^2\right\}^{1/2} \leq 1, \tag{12}$$

where $J_{\text{merge},0}=1°$, $J_{\text{split},0}=0.3$, $J_{a,0}=0.3$, and $J_{b,0}=0.3$ are acceptable values for the different types of errors. This is, however, dependent on the application and is here implemented as changeable parameters.

Finally, the impact of various parameter settings on $J = (1/N)\Sigma_i^N J_i$, where N is the number of tracks, is investigated for both test data sets. The sensitivity measure is defined as

$$S_{pa} = 0.5\left(\frac{|\Delta J_{+10\%}|}{J} + \frac{|\Delta J_{-10\%}|}{J}\right)\left(\frac{|\Delta x|}{x}\right)^{-1}, \tag{13}$$

where $\Delta J_{+10\%}$ and $\Delta J_{-10\%}$ are the changes in J when perturbing parameter $pa \pm 10\%$, and $|\Delta x|/x=0.1$, except for the parameters that are integers. To test the sensitivity to integer parameters, the parameter value is increased or decreased by one and $|\Delta x|/x=1/N_0$, where N_0 is the unperturbed value. A similar method was used to test the sensitivity to data association in Handegard *et al.* [2005, their Eq. (15)].

III. RESULTS

The performance of the algorithm is demonstrated by its ability to associate samples in the test-data sets to tracks. First the results from the full data sets are presented (Fig. 1). Then subset 1 from data set I is used to demonstrate the ability to track closely spaced targets as compared to a traditional SED algorithm. Finally, subset 2 from data set I is presented as an example where the tracking fails. Here the importance of the track quality algorithm is shown.

The ability of the method to associate samples into individual tracks is presented in Figs. 1(b) and 1(f). The parameters for the association method are specified in Table II, and the general parameters used for the tracking, i.e., to obtain the prediction, etc., are similar to those in Handegard *et al.* (2005, their Table V, case I).

By inspecting the intensity echogram of test-data set I [Fig. 1(a)], distinctive tracks can be distinguished by eye. When simultaneously looking at the anglegrams [Figs. 1(c) and 1(d)], the tracks are more clearly separable. Actually, the angles are remarkably stable over a track, even if the echo intensity for the track is low. When visually comparing the echograms and anglegrams with the classification image [Fig. 1(b)], it is seen that the tracks are well detected. The distinctive tracks are classified as good tracks, whereas dubious registrations are marked as low-quality tracks. The same can be seen in the results for test-data set II [Fig. 1(e)].

The tracking algorithm can be used to separate background reverberation samples and track samples. Here, background reverberation is defined as the signal from a nontargeted scatterer. The empirical distribution for intensity and angles for both background reverberation and signal samples are presented [Figs. 3(a) and 3(b), respectively]. There is an overlap between the signal and background reverberation distributions in intensity. This may be caused by the failure to detect the beginning of some of the low-quality tracks, which are thus being classified as background reverberation. Similarly, some background reverberation samples will be falsely associated with tracks. This is defined as association errors, see the following. When looking at the angle distributions, a typical "circular" distribution is seen for the targets [Fig. 3(b)]. If the targets were uniformly distributed within the beam with r degrees opening angle, the probability density along one angle, e.g., α, times the number of

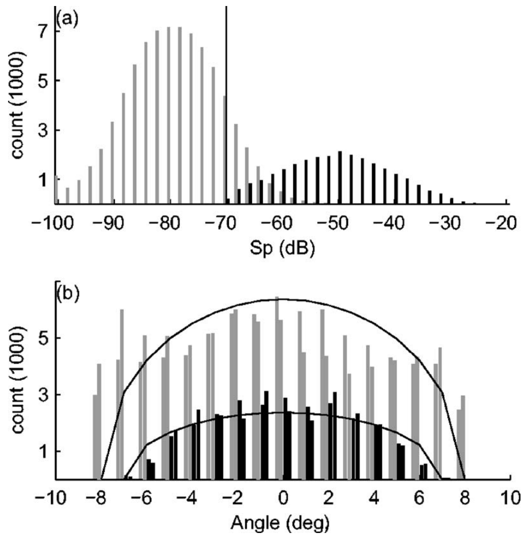

FIG. 3. The signal and background reverberation distributions. Signals are defined to be samples that belong to a track [see Fig. 1(b)], and background reverberation is defined to be samples more than two pixels away from a defined track. (a) The intensity distribution in S_p units (dB re m^2), where light gray bars are from background reverberation samples and black bars are from signal samples. The vertical line is the −70 dB threshold. (b) The angle distribution, where the light gray bars are background reverberation and black bars are signal. The first and second adjacent similarly colored bars are the alongship and athwart ship angles, respectively. The lines are the resulting angle distributions given uniformly distributed targets within $\alpha^2+\beta^2 \leq r^2$.

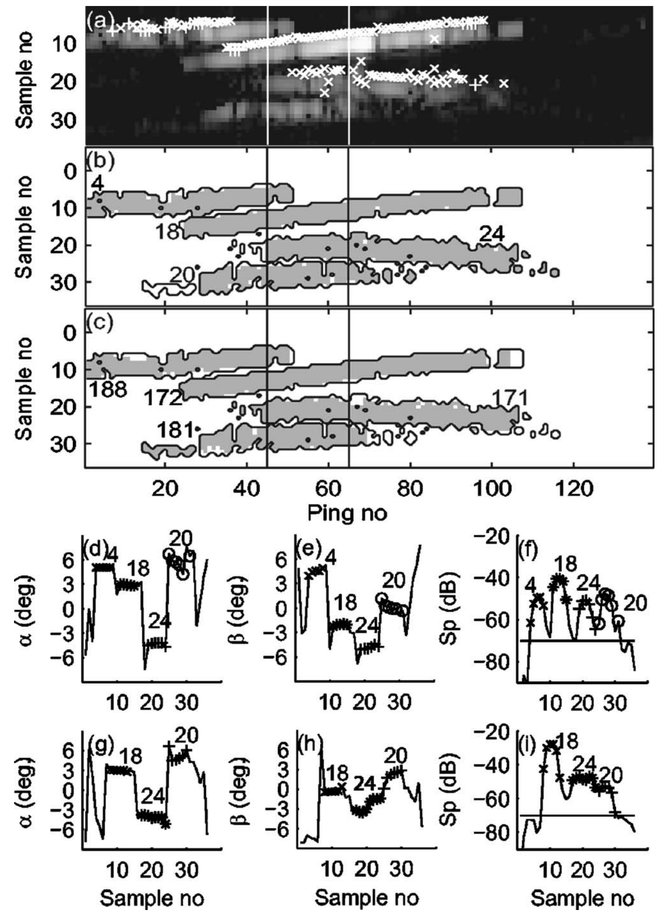

FIG. 4. Successful tracking of closely spaced targets. (a) The intensity echogram, where the white "+" and "×" denote the SED targets from EK60 and SONAR 5, respectively. The white vertical lines are the examples shown in (d)–(f) and (g)–(i), respectively. (b), (c) The forward and backward data association, respectively. Numbers indicate track numbers. The outlines denote the combination of the forward and backward tracking. Panels (d)–(f) and (g)–(i) show the intensity and angles for the samples indicated by vertical lines in (a)–(c). (×), (*), (+), and (○); Samples that have been associated with different tracks. The track numbers are printed above.

samples would be given by $y \sim N\sqrt{1-\alpha^2/r^2}/2\pi$, where N is the total number of samples. This seems to fit the results well, indicating that the targets $(r=7°)$ were indeed randomly positioned across the beam. In the case of the background reverberation samples, the circular distribution is a less good fit (using $r=8°$). This distribution seems to be a combination of a uniform and a circular distribution. The uniform part is analogous to the model assumption in Kieser *et al.* [2000, their Eq. (4)]. The circular distribution component may originate from nondetected tracks or other nonfish scatters in the water column.

A subset of test-data set I, where closely spaced data are successfully tracked, is used to compare the ability of the tracker against the traditional SED, and to present the combination of forward and backward tracks (Fig. 4). The algorithm detects four tracks, but the EK60 SED does not accept many targets in this case. This may be beneficial when estimating TS, but is not necessarily an advantage for tracking purposes. SONAR 5 accepts more targets, but may also include more false targets. This is not so crucial, since the tracking algorithm would reject the false targets. However, both methods present several missing detections along a track. To illustrate the information used by the SED algorithm, the data contained in two separate pings are presented [See Figs. 4(d)–4(f) and Figs. 4(g)–4(i)]. To separate the targets, the conventional SED initially attempts to identify the peaks based only on the echo intensities. This may be possible in the first example [Fig. 4(f)] but is clearly not possible in the second example [Fig. 4(i)]. Success would also depend on the SED settings (Table I). If the threshold is set too low, several targets will be within the window and are thus rejected. However, when taking the angles into account, the tracks are separable. Tracks 20 and 24 are clearly separated by the alongship angles [Fig. 4(g)]. Without taking the angles into consideration, it would not be possible to properly track these signals. This is also demonstrated by the complete failure of both SED algorithms to detect track 20 [Fig. 4(a)]. The combination of forward and backward tracks are presented in Figs. 4(b) and 4(c). If the tracks meet the criteria of overlap i.e., $J_a < 0.25$ and $J_b < 0.25$ in this case, the forward and backward runs are combined into a single merged track. The tracks in this subsample meet the stated criteria, and are successfully merged [Fig. 4(b)]. Note that the track numbers are different in the forward and backward case.

When the density is increasing, the limitations inherent in the split-beam principle will cause any tracking algorithm to fail. The track quality algorithm is thus an important part of the tracker, as it flags the cases where the tracker fails. Subset 2 of test data set I, where the algorithm fails, is used as an example (Fig. 5). Note that it is also difficult to determine tracks by visually inspecting the echogram and anglegrams [Figs. 1(a), 1(c), and 1(d), inside second box]. Since

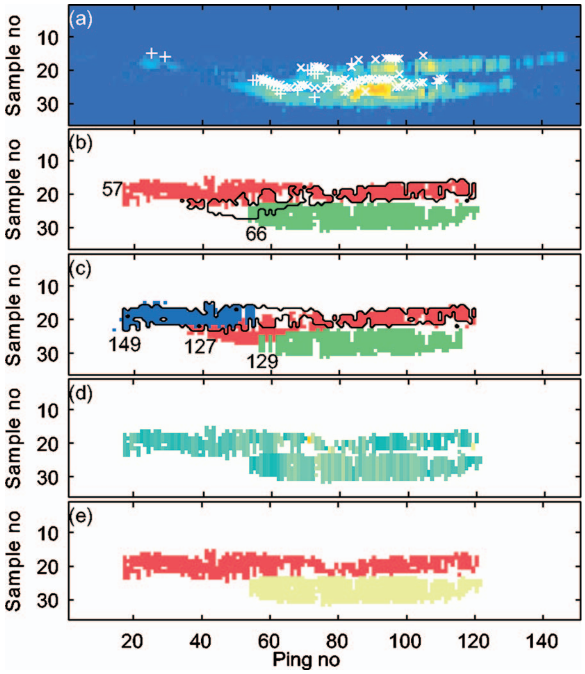

FIG. 5. Example of unsuccessful tracking. (a) The intensity echogram. The color scale is similar to Fig. 1(a). (b), (c) The results from the forward and backward tracking, respectively, on which J_a and J_b are based. Different colors indicate different tracks. Track 57 in the forward run (b) is taken as an example. The boundary from this track is transported to (c), i.e., the result from the backward run. It is seen that backward track 127 covers the largest proportion of this boundary, i.e., 46%. The J_a value is then $J_a=1-0.46=0.54$. Then the boundary of the backward track 127 is transported to the forward case panel (b). Track 57 covers 66% of this area, and thus $J_b=1-0.66=0.34$. (d) $J_{\mathrm{merge},ik}/J_{\mathrm{merge},0}$ with the color-scale range from [0 2], similar to Figs. 1(b) and 1(f). (e) The resulting quality of the tracks, with the color scale range from [0 2], similar to (d).

the forward and backward tracking do not agree [Figs. 5(b) and 5(c)], and the merge and track-split errors are high (Table III), the algorithm marks the tracks as low quality. Further, the SED targets of the two algorithms are inconsistent in this case, and tracking these would yield doubtful results. The classification is done for both test-data sets [Figs. 1(b) and 1(f), Table III].

Sensitivity. The sensitivity test investigates the impact of

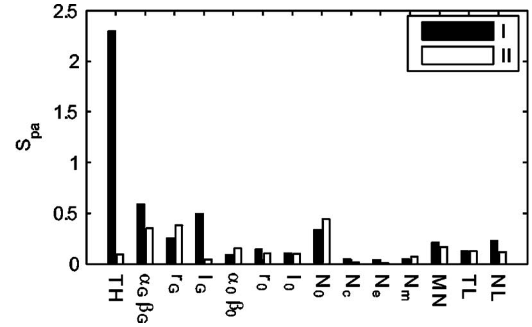

FIG. 6. The sensitivity S_{pa} for the different parameters, for data sets I and II, respectively.

parameter values on the track quality, giving an indication of which parameters are most important in the algorithm. The sensitivity for both test-data sets is given in Fig. 6. In general, the threshold, TH, is most important, followed by the gate and track initiation parameters. The lowest sensitivity is found in the track-termination parameters (N_c, N_e, and N_m). The sensitivity to the track-rejection parameters (MN, TL, and NL) is low, but this result depends on the initial parameter setting. If they are set to reject a large portion of the tracks, the rejection parameters become more important. Consequently, this test should be interpreted with care.

IV. DISCUSSION

The failure of the SED algorithm when tracking inside dense fish registrations was the motivation for this work, but there are other reports of problems with the SED procedure. Cronkite *et al.* (2004, their Sec. 4.3) discuss the problem of detecting closely spaced targets. They argue that the poor detection of closely spaced targets is caused by the echosounder SED algorithm, rather than acoustic shadowing within the aggregation. The inadequacy of the SED algorithm is thus not unique to the test cases reported here. In addition, the focus in fisheries acoustics has shifted from addressing technical problems like calibration, etc., to a more biological perspective, addressing behavioral considerations. This shift is evident in the Proceedings of the International

TABLE III. The first column indicates the test set I or II, and, where applicable, subset 1 or 2. The subsets refer to the boxes in Fig. 1(a), and Figs. 5 and 4, respectively. Where no track number is given, the mean of the respective data is presented, i.e., I,1 indicates the mean values from the tracks in subset 1 in test set I. I and II indicate the mean values of the full test sets. TrNoF and TrNoB indicate track numbers in the forward and backward cases, respectively, L_i is the track length (or mean length for the mean values) for the forward case, J_i (or J for the mean values), J_a, J_b, J_{merge}, and J_{split} are the quality measures defined in Sec. II C.

	TrNoF	TrNoB	L_i	J_i	J_a	J_b	J_{merge}	J_{split}
I,1	4	188	51	0.672	0.120	0.079	0.014	0.029
I,1	18	172	83	0.638	0.080	0.026	0.015	0.018
I,1	20	181	56	1.183	0.191	0.194	0.023	0.052
I,1	24	171	72	0.784	0.123	0.078	0.017	0.045
I,1			66	0.819	0.129	0.094	0.017	0.036
I,2	57	127	104	2.247	0.535	0.340	0.034	0.063
I,2	66	129	68	0.901	0.182	0.060	0.017	0.096
I,2			86	1.574	0.359	0.200	0.026	0.079
I			51	1.419	0.237	0.244	0.020	0.065
II			60	1.858	0.312	0.401	0.016	0.189

Council for Exploration of the Sea (www.ices.dk), which has sponsored symposia on fisheries acoustics (Craig, 1984; Karp, 1990; MacLennan *et al.*, 2003; Margetts, 1977; Massé *et al.*, 2003; Simmonds, 1996). Consequently, an improved methodology for addressing these questions is valuable.

Different applications make different demands on the tracking and detection algorithms. The SED algorithm was originally designed to estimate the TS of species of interest, and achieves this by rejecting low-quality targets (Soule *et al.*, 1996). By accepting only the high-quality-single targets, many pings may not register along the track in the subsequent tracking. This adversely results in split tracks and position errors, which in turn make the estimation of target velocity and position difficult. Apart from that, there are other problems with rejecting weak and low-quality targets before tracking. For example, estimates of target strength are improved when there are samples over several pings from the same fish (Ehrenberg and Torkelson, 1996; Foote *et al.*, 1984), and tracking can be used to obtain behavioral observations relevant to the target strength estimation (Chu *et al.*, 2003; McQuinn and Winger, 2003). Consequently, improving our ability to track single individuals may lead to better TS estimates, and if bias in intensity is a concern, the quality could be controlled by track quality parameters like the J_{merge}, cf. the following discussion of track quality. Another effect of the traditional approach is that weak and low-quality targets are undetected, which is a problem when addressing the interindividual behavior issues mentioned in Sec. I. Here it is crucial that low-quality tracks are detected, to avoid false nearest-neighbor pairing. This is also important when investigating the spatial distribution from single-target observations, as in, e.g., Pedersen (1996); Trenkel *et al.* (2004). Consequently, the method presented here improves the feasibility of experiments that rely on our ability to resolve single targets, including TS estimation.

Target tracking is a large field with an extensive literature, and several methods have been described, see, e.g., Blackman and Popoli (1999) as a general reference. Other data-association methods include multiple-hypothesis tracking. This approach delays the decision on data association for several pings, and keeps track of the most likely target associations. This results in several combinations (hypotheses) of the targets. This is the recommended data-association method according to Blackman and Popoli (1999, Chap. 6). However, keeping track of several track-combination hypotheses when working with echo samples, as opposed to single targets, would yield a vast number of combinations. It is possible that the method could be refined to fit this approach, but the complexity would increase. Other approaches includes particle filtering, e.g., the probability-hypothesis-density (PHD) method. The PHD filter has been implemented for forward-scan sonar images (Clark and Bell, 2005), and one advantage of this approach is its ability to filter signals in high clutter, reducing the number of spurious measurements. However, data association, the main consideration in this paper, is not presently addressed in the PHD method.

The novelty in the present work is the track-before-detect approach. This implies the use of angle samples in the detection, not only for rejection in the SED algorithms and in subsequent tracking. This is achieved by treating each sample above a threshold as a single target, and allowing for several associations of samples to each prediction (track). The approach is simple, but some further consideration of why it works may be appropriate. Humans have a remarkable capability to extract information from images, and that is one of the reasons that tracking targets in intensity echograms by eye often performs better than automatic tracking. However, when we include both anglegrams and existing track predictions in addition to the intensity echogram, our ability is less superior because we have to interpret the information in several images simultaneously. The computer has no problem in handling this multidimensionality.

A. Parameter sensitivity and track quality

The method is very flexible, and calls for caution when setting the parameters. In general, one should start with the most sensitive parameters and progress to the less sensitive parameters. The threshold should initially be set low to not miss any targets, and should subsequently be increased if necessary. The N_n parameter indicating the number of samples needed to initiate a track should be approximately the number of samples per ping from each target (5 in test data I). This is dependent on the sampling interval, the pulse length, and the target size range. The track-initiation gate range parameter, r_0, should be set slightly higher than the resolution in range (9.4 and 1.2 cm, for test data I and II, respectively). The track gate, G, depends on the fish behavior, the background reverberation, and the density. The track-termination and track-rejection parameters should initially be set high and then decreased, if necessary. After the initial settings are decided, a subsample of the data should be used for tuning the parameters. The parameters, G and G_0 should be tuned first. A larger initiation gate starts the tracks earlier, but potentially gives more false targets. If the track-initiation gate is narrowed too much, track-split errors in range may occur. If the track gate is increased, more rapid changes in behavior may be detected but several targets may be erroneously associated within one track, both in time and range. If the track gate is decreased, tracks may split and rapid changes in behavior will be undetected, but there will be less false associations. The track-termination and track-rejection parameters should be set to terminate and reject more tracks if the gate tuning does not improve the performance.

The performance of the tracker depends on the parameter values, and the above-outlined setting procedure involves subjectivity. An important aspect of the track-quality algorithm is to remove some of this subjectivity. As mentioned earlier, the definition of high or low quality may depend on the application, and these trade-offs can be achieved by different weights on the various quality measures. Further, a low-quality track may convert to a high-quality track by tuning the tracking parameters correctly, while the definition of track quality remains the same. Consequently, the track quality indicates the comparative success of the different parameter settings, but is also an absolute (as opposed to relative) measure of the track quality. This distinction is important because it gives us the possibility to assess whether tracking is feasible or not in a given situation, beyond the information on how well the parameters are set.

Although track quality measures have been established, the ultimate test is to visually compare the automatic classification into tracks with the appearance of the echogram and the anglegrams. The value of carefully inspecting these should not be underestimated, because humans are highly skilled at extracting information from images. Some researchers argue that manual tracking is better and more accurate than automatic tracking. Although this may be true in some cases, the manual approach is less consistent. Manual tracking may yield different results depending on who scrutinizes the data. Algorithms with given parameter settings do not have this problem.

B. Track estimation

An important part of any tracking system is the track-estimation process. Here, track estimation is defined as the information one can obtain from the samples comprising a single track, e.g., the estimated positions, the corresponding velocities, TS, etc. For example, if swimming velocities are required, simply dividing the distance between target fixes by the time difference is not good enough, because the observation errors are ignored, cf. Mulligan and Chen (2000) for a convincing illustration. Although this paper focuses on data association, a short discussion of different track estimation techniques is included.

The Kalman filter is a common method for estimating speed and positions in tracking applications. This is a powerful tool when real-time tracking is required, e.g., in the data association process when predictions are needed or when tracking airplanes or missiles. When estimating fish swimming trajectories, however, we can estimate the tracks after association. This enables us to use a whole suite of estimation techniques. Several methods have been tested on split-beam data in Handegard *et al.* (2005). Both smoothing splines and Kalman smoothing (Kalman smoothing traverse the Kalman filter estimates backwards to reduce dependence of the initial conditions) were found to work well for position estimates, but the Kalman smoother failed to estimate the velocities. In the test cases presented here, however, the Kalman smoother produced sensible results. If the process and measurement errors are well known, the Kalman smoother is an appropriate tool since it separates the process and observation errors, i.e., it reduces the number of *ad hoc* parameters. Another approach is to use smoothing splines where the smoothing is set by cross validation. For the test data in this paper, the cross-validation method detected periodicity in the position estimates. This has the potential to give grossly overestimated swimming-speed estimates if not corrected for. The importance of plotting the tracks to assess this effect should not be underestimated. However, the periodicity is believed to be caused by the tail-beat frequency of individual fish, and this could potentially be associated with the swimming speed (Bainbridge, 1960).

Another aspect, not addressed in this paper, is the quality of the angle measurements in each sample. This should be considered when estimating fish position and velocity. For example, low signal-to-noise ratio gives higher variability in the angles, but may also bias them toward the center of the beam (Kieser *et al.*, 2000). This is especially important when using sonars close to boundaries, as would apply in a riverine environment or with horizontal transmissions near the bottom or the water surface.

V. CONCLUSIONS

The main advantages of tracking samples directly without prior target detection are simplicity and efficiency. The process is simple, because no prior detection is necessary as the process of tracking and detection is done in one step. The efficiency is improved by the target angles being utilized along with the intensity and range data, as opposed to the conventional SED algorithm that works on intensity and range only. The benefit of this approach has been clearly demonstrated.

The combination of the improved data association and the quality control substantially improves our ability to investigate the behavior of closely spaced single targets, providing the means to learn more about the behavior of the individual animals within aquatic ecosystems.

ACKNOWLEDGMENTS

This work was carried out during a stay at the University of Washington and NOAA Alaska Fisheries Science Center, Seattle, funded by the Norwegian Research Counsel under the Leiv Erikson program. I would like to thank Egil Ona and Lucio Calise for the test data sets I and II, respectively, Karl Øystein Gjelland for processing the SONAR 5 data, and Vidar Hjellvik, Alex De Robertis, and Patrick H. Ressler for comments on the manuscript.

[1] I use the term "anglegram" to describe a ping-by-ping display of targets which are color-coded to indicate one of the bearing angles.

[2] Personal communication, based on camera observations of fish in a tank.

Aoki, I. (**1982**). "A simulation study on the schooling mechanism in fish," Bull. Japanese Soc. Sci. Fisheries **48**, 1081–1088.

Arrhenius, F., Benneheij, B. J., Rudstam, L. G., and Boisclair, D. (**2000**). "Can stationary bottom split-beam hydroacoustics be used to measure fish swimming speed in situ?," Fisheries Research **45**, 31–41.

Bainbridge, R. (**1960**). "Speed and stamina in three fish," J. Exp. Biol. **37**, 129–153.

Balk, H., and Lindem, T. (**2000**). "Improved fish detection in data from split-beam transducers," Aquatic Living Resources **13**, 297–303.

Blackman, S. S., and Popoli, R. (**1999**). *Design and Analysis of Modern Tracking Systems* (Artech House, Boston).

Brede, R., Kristensen, F. H., Solli, H., and Ona, E. (**1990**). "Target tracking with a split-beam echo sounder," Rapp. P.-v. Reun.-Cons. Int. Explor. Mer **189**, 254–263.

Breder, C. M. J. (**1954**). "Equations descriptive of fish schools and other animal aggregations," Ecology **35**, 361–370.

Cech, M., and Kubecka, J. (**2002**). "Sinusoidal cycling swimming pattern of reservoir fishes," J. Fish Biol. **61**, 456–471.

Chu, D., Jech, J. M., and Lavery, A. (**2003**). "Inference of geometrical and behavioural parameters of individual fish from echo-trace-analysis," Deep-Sea Res., Part I **50**, 515–527.

Clark, D., and Bell, J. (**2005**). "Bayesian multiple target tracking in forward scan sonar images using the phd filter," IEE Proc., Radar Sonar Navig. **152**, 327–334.

Craig, R. ed. (**1984**). ICES Symposium on Fisheries Acoustics, Bergen, Norway, 1982, Rapp. P.-v. Reun.-Cons. Int. Explor. Mer **184**.
Cronkite, G. M., Enzenhofer, H. J., and Gray, A. P. (**2004**). “Split-beam sonar observations of targets as an aid in the interpretation of anomalies encountered while monitoring migrating adult salmon in rivers,” Aquatic Living Resources **17**, 1–12.
De Robertis, A., Schell, C., and Jaffe, J. (**2003**). “Acoustic observations of the swimming behaviour of the euphasiid *Euphasia pacifica* Hansen,” ICES J. Mar. Sci. **60**, 885–898.
Ehrenberg, J. E., and Torkelson, T. C. (**1996**). “Application of dual-beam and split-beam target tracking in fisheries acoustics,” ICES J. Mar. Sci. **53**, 329–334.
Enzenhofer, H. J., Olsen, N., and Mulligan, T. J. (**1998**). “Fixed-location riverine hydroacoustics as a method of enumerating migrating adult pacific salmon: Comparison of split-beam acoustics vs. visual counting,” Aquatic Living Resources **11**, 61–74.
Foote, K. G. (**1996**). “Coincidence echo statistics,” J. Acoust. Soc. Am. **99**, 266–271.
Foote, K. G., Aglen, A., and Nakken, O. (**1986**). “Measurement of fish target strength with a split-beam echo sounder,” J. Acoust. Soc. Am. **80**, 612–621.
Foote, K. G., Kristensen, F. H., and Solli, H. (**1984**). “Trial of a new, split-beam echo sounder,” Coun. Meet. Int. Coun. Explor. Sea B:21, Copenhagen, Denmark.
Genin, A., Jeffe, J. S., Reef, R., Richter, C., and Franks, P. J. S. (**2005**). “Swimming against the flow: A mechanism of zooplankton aggregation,” Science **308**, 860–862.
Gjelland, K. Y., Bøhn, T., Knudsen, F. R., and Amundsen, P.-A. (**2004**). “Influence of light on the swimming speed og coregonids in subarctic lakes,” Ann. Zool. Fennici **41**, 137–146.
Handegard, N. O., Michalsen, K., and Tjøstheim, D. (**2003**). “Avoidance behaviour in cod (*gadus morhua*) to a bottom-trawling vessel,” Aquatic Living Resources **16**, 265–270.
Handegard, N. O., Patel, R., and Hjellvik, V. (**2005**). “Tracking individual fish from a moving platform using a split-beam transducer,” J. Acoust. Soc. Am. **118**, 2210–2223.
Handegard, N. O., and Tjøstheim, D. (**2005**). “When fish meets a trawling vessel: Examining the behaviour of gadoids using a free floating buoy and acoustic split-beam tracking,” Can. J. Fish. Aquat. Sci. **62**, 2409–2422.
Huse, I., and Ona, E. (**1996**). “Tilt angle distribution and swimming speed of overwintering norwegian spring spawning herring,” ICES J. Mar. Sci. **53**, 863–873.
Huth, A., and Wissel, C. (**1992**). “The simulation of the movement of fish schools,” J. Theor. Biol. **156**, 365–385.
Jaffe, J. S. (**1999**). “Target localization for a three-dimensional multibeam sonar imaging system,” J. Acoust. Soc. Am. **105**, 3168–3175.
Jaffe, J. S., Ohman, M. D., and De Robertis, A. (**1999**). “Sonar estimates of daytime activity levels of *Euphausia pacifica* in Saanich Inlet,” Can. J. Fish. Aquat. Sci. **56**, 2000–2010.
Jaffe, J. S., Reuss, E., McGehee, D., and Chandran, G. (**1995**). “FTV, a sonar for tracking macrozooplankton in 3-dimensions,” Deep-Sea Res., Part I **42**, 1495–1512.
Karp, W., ed. (**1990**). ICES Symposium on Developments in Fisheries Acoustics, Seattle, WA, 1987, Rapp. P.-v. Reun. Cons. Int. Explor. Mer **189**.
Kieser, R., Mulligan, T., and Ehrenberg, J. (**2000**). “Observation and explanation of systematic split-beam angle measurement errors,” Aquatic Living Resources **13**, 275–281.
Klevjer, T. A., and Kaartvedt, S. (**2003**). “Split-beam target tracking can be used to study the swimming behaviour of deep-living plankton in situ,” Aquatic Living Resources **16**, 293–298.
MacLennan, D. N., Massé, J., and Gerlotto, F., eds. (**2003**). Sixth ICES Symposium on Acoustics in Fisheries and Aquatic ecology, Part 1, Montpellier, France, 2002, ICES J. Mar. Sci. **60**.
Margetts, A., ed. (**1977**). ICES Symposium on Hydro-Acoustics in Fisheries Research, Bergen, Norway, 1973, Rapp. P.-v. Reun. Cons. Int. Explor. Mer **170**.
Massé, J., Gerlotto, F., and MacLennan, D. N., eds. (**2003**). Sixth ICES Symposium on Acoustics in Fisheries and Aquatic ecology, Part 2, Montpellier, France, Aquatic Living Resources **16**.
McKinstry, C. A., Simmons, M. A., Simmons, C. S., and Johnson, R. L. (**2005**). “Statistical assessment of fish behavior from split-beam hydroacoustic sampling,” Fisheries Research **72**, 29–44.
McQuinn, I., and Winger, P. (**2003**). “Tilt angle and target strength: Target tracking of atlantic cod (gadus morhua) during trawling,” ICES J. Mar. Sci. **60**, 575–583.
Mulligan, T., and Chen, D. (**2000**). “Comment on ‘can stationary bottom split-beam hydroacoustics be used to measure fish swimming speed in situ?’ by Arrhenius *et al.*,” Fisheries Research **49**, 93–96.
Mulligan, T. J., and Chen, D. G. (**1998**). “A split-beam echo counting model: Development of statistical procedures,” ICES J. Mar. Sci. **55**, 905–917.
Mulligan, T. J., and Kieser, R. (**1996**). “A split-beam echo-counting model for riverine use,” ICES J. Mar. Sci. **53**, 403–406.
Ona, E. (**1994**). “Recent developments of acoustic instrumentation in connection with fish capture and abundance estimation,” in *Marine Fish Behaviour in Capture and Abundance Estimation*, edited by A. Fernö and S. Olsen (Fishing News Books, Oxford, UK), pp. 200–214.
Ona, E., ed. (**1999**). “Methodology for Target Strength Measurements,” ICES Cooperative Research Report (International Council for the Exploration of the Sea), Vol. **235**.
Parr, A. E. (**1927**). “A contribution to the theoretical analysis of the schooling behaviour of fishes,” Occasional Papers of the Bingham Oceanographic Collection **1**, 1–32.
Pedersen, J. (**1996**). “Discrimination of fish layers using the three-dimensional information obtained by a split-beam echo-sounder,” ICES J. Mar. Sci. **53**, 371–376.
Reynolds, C. W. (**1987**). “Flocks, herds, and schools: A distributed behavioural model,” Comput. Graphics **21**, 25-34.
Sakai, S. (**1973**). “A model for group structure and its behaviour,” Biophysics (Engl. Transl.) **13**, 82–90.
Schell, C., and Jaffe, J. S. (**2004**). “Experimental verification of an interpolation algorithm for improved estimates of animal position,” J. Acoust. Soc. Am. **116**, 254–261.
Simmonds, E. J., ed. (**1996**). ICES Symposium on Fisheries and Plankton Acoustics, Aberdeen, Scotland, 1995, ICES J. Mar. Sci. **53**.
Soule, M., Hampton, I., and Barange, M. (**1996**). “Potential improvements to current methods of recognizing single targets with a split-beam echosounder,” ICES J. Mar. Sci. **53**, 237–243.
Torgersen, T., and Kaartvedt, S. (**2001**). “In situ swimming behaviour of individual mesopelagic fish studied by split-beam echo target tracking,” ICES J. Mar. Sci. **58**, 346–354.
Trenkel, V. M., Godø, O. R., Handegard, N. O., and Patel, R. (**2004**). “Studying the relationship between spatial fish distributions and trawl catches,” Coun. Meet. Int. Coun. Explor. Sea R:26, Copenhagen, Denmark.
Xie, Y. (**2000**). “A range-dependent echo-association algorithm and its application in split-beam sonar tracking of migratory salmon in the fraser river watershed,” IEEE J. Ocean. Eng. **25**, 387–398.